

HUPD-9713
June 1997

Determination of the CKM unitarity triangle by $B \rightarrow X_d \ell^+ \ell^-$ decay

L. T. Handoko *

Department of Physics, Hiroshima University
1-3-1 Kagamiyama, Higashi Hiroshima - 739, Japan

Abstract

I examine a possibility to extract the angle γ of the Cabibbo-Kobayashi-Maskawa unitarity triangle by the inclusive $B \rightarrow X_d \ell^+ \ell^-$ decay. An independent information for the angle is expected from the non-trivial contribution induced in $u\bar{u}$ and $c\bar{c}$ loops. The contributions induce CP asymmetry which has high sensitivity to the angle γ in the whole dilepton invariant mass region. Particularly, in the low dilepton invariant mass region, the sensitivity is also recognized in the branching-ratio with any dilepton final states and the lepton polarization asymmetry with dimuon final state. In the high dilepton invariant mass region, the sensitivity is tiny in all measurements with the exception of the CP asymmetry, that make them to be good probes to confirm the measurement of $V_{td}^* V_{tb}$ in addition to the present data from $B_d^0 - \bar{B}_d^0$ mixing. The decay rate and asymmetries are examined in the Standard Model with taking into account the long-distance contributions due to vector-mesons as well as its momentum dependences that would reduce the long-distance backgrounds in the channel.

*On leave from P3FT-LIPI, Indonesia. E-mail address : handoko@theo.phys.sci.hiroshima-u.ac.jp

1 Introduction

The hope that $B \rightarrow X_s \ell^+ \ell^-$ decay will be within experimental reach in the near future [1] encourage me to consider $B \rightarrow X_d \ell^+ \ell^-$ decay. Both decays are important probes of the effective Hamiltonian governing the flavor-changing neutral current (FCNC) transition $b \rightarrow q \ell^+ \ell^-$ ($q = s, d$) in the Standard Model (SM) as written below [2]

$$\mathcal{H}_{\text{eff}} = \frac{G_F \alpha}{\sqrt{2} \pi} V_{tq}^* V_{tb} \left\{ C_9^{\text{eff}} [\bar{q} \gamma_\mu L b] [\bar{\ell} \gamma^\mu \ell] + C_{10} [\bar{q} \gamma_\mu L b] [\bar{\ell} \gamma^\mu \gamma_5 \ell] - 2 C_7^{\text{eff}} \left[\bar{q} i \sigma_{\mu\nu} \frac{\hat{q}^\nu}{\hat{s}} (R + \hat{m}_q L) b \right] [\bar{\ell} \gamma^\mu \ell] \right\}. \quad (1)$$

where $L/R \equiv (1 \mp \gamma_5)/2$, q^μ denotes four-momentum of the dilepton, $s = q^2$. Notation with hat on the top means it is normalized with m_b .

Theoretically, the most important interest in the $b \rightarrow d \ell^+ \ell^-$ decay is, the matrix element contains un-negligible terms induced by continuum part of $u\bar{u}$ and $c\bar{c}$ loops proportional to $V_{ud}^* V_{ub}$ and $V_{cd}^* V_{cb}$ [4]. These terms should give non-trivial contributions in the Wilson coefficient C_9^{eff} which induce CP violation in the channel. I call the contribution as CP violation factor (C_9^{CP}) throughout this paper. I will show that it can be utilized to determine the length x and the angle γ of the Cabibbo-Kobayashi-Maskawa (CKM) unitarity triangle in Fig. 1 at once. In this meaning, for example, the radiative $B \rightarrow X_d \gamma$ decay is not so useful since it gives only information for the length x that have already been measured well in the $B_d^0 - \bar{B}_d^0$ mixing. On the other hand, in the $b \rightarrow s \ell^+ \ell^-$ decay, C_9^{CP} is strongly suppressed due to the GIM mechanism. Generally, rare B decays are clean processes to extract the CKM matrix elements, because non-perturbative effects in the decays are possibly tiny, less than few percents as shown in [3] by using heavy-quark effective theory approach¹. In the analysis, I also utilize the experiment result of x_d in the $B_d^0 - \bar{B}_d^0$ mixing.

The purpose of this paper is to show a possibility to give an independent mea-

¹Remark that the approach is reliable only in the low dilepton mass region, but it is sufficient to justify the statement since in the high dilepton mass region the perturbative calculation is good.

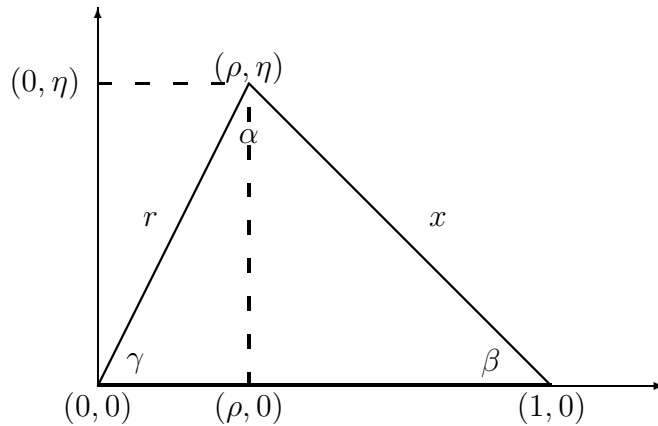


Figure 1: The CKM unitarity triangle on the $\rho - \eta$ plane.

surement for the angle γ of CKM unitarity triangle in the SM by observing the channel. The calculation is done with taking into account the q -dependence in the long-distance (LD) contributions due to the vector mesons [7]. It is well known that including the q -dependence, which has not been considered in the previous papers, will reduce the background due to LD contributions [8].

This paper is organized as follows. First I briefly describe the non-trivial contributions due to resonance and continuum parts of $u\bar{u}$ and $c\bar{c}$ loops which induce C_9^{CP} . Next I consider the phenomenology of the contributions and its relation with the CKM unitarity triangle. Before going to summary, I analyse the decay rate and asymmetries, i.e. forward-backward (FB) asymmetry ($\bar{\mathcal{A}}_{\text{FB}}$), CP asymmetry ($\bar{\mathcal{A}}_{\text{CP}}$) and lepton-polarization (LP) asymmetry ($\bar{\mathcal{A}}_{\text{LP}}$) in the channel.

2 CP violation factor

The effective Hamiltonian in Eq. (1) describes both inclusive $b \rightarrow q \ell^+ \ell^-$ decays by replacing q with s or d quark respectively. In the SM, the QCD corrected Wilson coefficients enter in the physical decay amplitude above have been calculated up to next-to leading order (NLO) for C_9^{eff} and leading order (LO) for C_7^{eff} [5], while C_{10} does not receive any correction at all. Some corrections due to continuum parts of $u\bar{u}$ and $c\bar{c}$ continuums and the resonances of the vector-mesons will enter only in the coefficient C_9^{eff} . Remind that the contribution of $u\bar{u}$ loop in C_7^{eff} is suppressed due to the GIM mechanism [10].

Before going to give C_9^{eff} , related with $u\bar{u}$ and $c\bar{c}$ loops, let me mention the operators govern the $b \rightarrow q u^i \bar{u}^i$ processes,

$$\mathcal{O}_1 = (\bar{q}_\alpha \gamma_\mu L b_\alpha) \sum_{i=1,2} (\bar{u}_\beta^i \gamma^\mu L u_\beta^i), \quad (2)$$

$$\mathcal{O}_2 = (\bar{q}_\alpha \gamma_\mu L b_\beta) \sum_{i=1,2} (\bar{u}_\beta^i \gamma^\mu L u_\alpha^i), \quad (3)$$

after doing Fierz transformation. Here, $u^1 = u$, $u^2 = c$ and the lower suffixes denote the color. For $q = s$, $u\bar{u}$ loop contribution can be ignored [2, 5], while for $q = d$ the situation is quite different. The reason is, both operators above are proportional to the CKM matrix element $V_{u^i q}^* V_{u^i b} / V_{tq}^* V_{tb}$ if we normalize the amplitude with $V_{tq}^* V_{tb}$ as usual, then

$$\left| \frac{V_{u^i s}^* V_{u^i b}}{V_{ts}^* V_{tb}} \right| \sim \begin{cases} O(\lambda^2) & , \quad u^i = u \\ O(1) & , \quad u^i = c \end{cases}, \quad (4)$$

for the former channel, and

$$\left| \frac{V_{u^i d}^* V_{u^i b}}{V_{td}^* V_{tb}} \right| \sim \begin{cases} O(1) & , \quad u^i = u \\ O(1) & , \quad u^i = c \end{cases}, \quad (5)$$

for the later one. λ is a parameter in Wolfenstein parametrization of CKM matrix [6] and the world average is $\lambda \sim 0.22$ [11].

Involving the continuum as well as resonance parts of $u\bar{u}$ and $c\bar{c}$ loops and NLO QCD correction into the calculation gives

$$C_9^{\text{eff}} = C_9^{\text{NLO}} \left[1 + \frac{\alpha_s(\mu)}{\pi} \omega(\hat{s}) \right] + C_9^{\text{con}}(\hat{s}) + C_9^{\text{res}}(\hat{s}), \quad (6)$$

where

$$\begin{aligned} C_9^{\text{con}}(\hat{s}) &= \left[\left(1 + \frac{V_{uq}^* V_{ub}}{V_{tq}^* V_{tb}} \right) g(\hat{m}_c, \hat{s}) - \frac{V_{uq}^* V_{ub}}{V_{tq}^* V_{tb}} g(\hat{m}_u, \hat{s}) \right] \\ &\quad \times (3C_1 + C_2 + 3C_3 + C_4 + 3C_5 + C_6) \\ &\quad - \frac{1}{2} g(1, \hat{s}) (4C_3 + 4C_4 + 3C_5 + C_6) \\ &\quad - \frac{1}{2} g(0, \hat{s}) (C_3 + 3C_4) + \frac{2}{9} (3C_3 + C_4 + 3C_5 + C_6), \end{aligned} \quad (7)$$

$$\begin{aligned} C_9^{\text{res}}(\hat{s}) &= -\frac{16\pi^2}{9} (3C_1 + C_2 + 3C_3 + C_4 + 3C_5 + C_6) \\ &\quad \times \left[\left(1 + \frac{V_{uq}^* V_{ub}}{V_{tq}^* V_{tb}} \right) \sum_{V=\psi, \dots} F_V(\hat{s}) - \frac{V_{uq}^* V_{ub}}{V_{tq}^* V_{tb}} \sum_{V=\rho, \omega} F_V(\hat{s}) \right]. \end{aligned} \quad (8)$$

The readers should refer [5] for C_9^{NLO} and

$$\begin{aligned} \omega(\hat{s}) = & -\frac{2}{9}\pi^2 - \frac{4}{3}\text{Li}_2(\hat{s}) - \frac{2}{3}\ln \hat{s} \ln(1 - \hat{s}) - \frac{5 + 4\hat{s}}{3(1 + 2\hat{s})} \ln(1 - \hat{s}) \\ & - \frac{2\hat{s}(1 + \hat{s})(1 - 2\hat{s})}{3(1 - \hat{s})^2(1 + 2\hat{s})} \ln \hat{s} + \frac{5 + 9\hat{s} - 6\hat{s}^2}{6(1 - \hat{s})(1 + 2\hat{s})}, \end{aligned} \quad (9)$$

represents the $O(\alpha_s)$ correction from the one gluon exchange in the matrix element of \mathcal{O}_9 . The function $g(\hat{m}_{u^i}, \hat{s})$ which describes the continuum part of $u^i\bar{u}^i$ pair contribution is

$$\begin{aligned} g(\hat{m}_{u^i}, \hat{s}) = & -\frac{8}{9}\ln\left(\frac{m_b}{\mu}\right) - \frac{8}{9}\ln(\hat{m}_{u^i}) + \frac{8}{27} + \frac{16}{9}\frac{\hat{m}_{u^i}^2}{\hat{s}} - \frac{2}{9}\left(2 + \frac{4\hat{m}_{u^i}^2}{\hat{s}}\right)\sqrt{\left|1 - \frac{4\hat{m}_{u^i}^2}{\hat{s}}\right|} \\ & \times \left[\Theta\left(1 - \frac{4\hat{m}_{u^i}^2}{\hat{s}}\right) \left(\ln \frac{1 + \sqrt{1 - 4\hat{m}_{u^i}^2/\hat{s}}}{1 - \sqrt{1 - 4\hat{m}_{u^i}^2/\hat{s}}} - i\pi \right) \right. \\ & \left. + \Theta\left(\frac{4\hat{m}_{u^i}^2}{\hat{s}} - 1\right) 2 \arctan \frac{1}{\sqrt{4\hat{m}_{u^i}^2/\hat{s} - 1}} \right], \end{aligned} \quad (10)$$

$$g(0, \hat{s}) = \frac{8}{27} - \frac{8}{9}\ln\left(\frac{m_b}{\mu}\right) - \frac{4}{9}\ln \hat{s} + \frac{4}{9}i\pi. \quad (11)$$

In the resonance part C_9^{res} , I put the relative phase to be zero because of unitarity constraint in the Argand plot of the transition amplitude [7]. $F_V(\hat{s})$ is the Breit-Wigner resonance form

$$F_V(\hat{s}) = \frac{\hat{f}_V^2(\hat{s})/\hat{s}}{\hat{s} - \hat{m}_V^2 + i\hat{m}_V\hat{\Gamma}_V}. \quad (12)$$

$\hat{f}_V(\hat{s})$ describes the momentum dependence of coupling strength of vector interaction in $\gamma - V$ transition, i.e.

$$\langle 0 | \bar{u}^i \gamma_\mu u^i | V(q) \rangle \equiv f_V(q^2) \epsilon_\mu, \quad (13)$$

and has been derived as follows [8]

$$\frac{\hat{f}_V(\hat{s})}{\hat{f}_V(0)} = 1 + \frac{\hat{s}}{\hat{P}_V} [P'_V - P''_V(\hat{s})], \quad (14)$$

under an assumption that the vector-mesons are bound-states of the pair $u^i\bar{u}^i$. Here,

$$P''_V(\hat{s}) = \frac{\hat{m}_{u^i}^2}{4\pi^2\hat{s}} \left[-4 - \frac{5\hat{s}}{3\hat{m}_{u^i}^2} + 4 \left(1 + \frac{\hat{s}}{2\hat{m}_{u^i}^2} \right) \sqrt{\frac{4\hat{m}_{u^i}^2}{\hat{s}} - 1} \arctan \frac{1}{\sqrt{4\hat{m}_{u^i}^2/\hat{s} - 1}} \right], \quad (15)$$

Parameter	Vector-meson					
	ρ	ω	ψ	ψ'	ψ''	ψ'''
M_V (MeV)	768.5	781.94	3096.88	3686.00	3769.9	4040
$\Gamma_{e^+e^-}$ (keV)	6.77	0.6	5.26	2.14	0.26	0.75
Γ_V (MeV)	150.7	8.43	0.087	0.277	23.6	52
$P_V''(\hat{m}_V^2)$	-0.00243	-0.00243	-0.02734	-0.01463	-0.01374	-0.01153
\hat{P}_V	0.01339	0.01387	0.01577	0.01830	0.01885	0.02080
$\hat{f}_V(0)$	0.00662	0.00202	0.01795	0.01487	0.00536	0.01010

Table 1: The experimental (central) values for each vector-meson under consideration (upper table) and the determined constants under these values (lower table).

is obtained from a dispersion relation involving the imaginary part of quark-loop diagram, while P_V and P_V' are the subtraction constants. Kinematically the above interpolation equation of \hat{f}_V is valid only for $0 \leq \hat{s} \leq \hat{m}_V^2$ region. For $\hat{s} > \hat{m}_V^2$ region I take same assumption with [8], that is $\hat{f}_V(\hat{s} > \hat{m}_V^2) = \hat{f}_V(\hat{m}_V^2)$. In principle, the ratio in Eq. (14) should be obtained from the known data of V production cross-section by off-shell and on-shell photons.

The subtraction constants in Eq. (14) are written in the lower table of Tab. (1) for each vector meson. The results are determined by using the data in the upper table, putting $m_V \sim (2m_{u^i})$ and $P_V' = 0.043$ for all V 's. Unfortunately, there is no data of photoproduction for higher excited states of ψ , so let me use same average value $|\hat{f}_V(0)/\hat{f}_V(\hat{m}_V^2)| \sim 0.35$ for $V = \psi, \psi', \psi'', \psi'''$ and $|\hat{f}_V(0)/\hat{f}_V(\hat{m}_V^2)| \sim 0.92$ for $V = \rho, \omega$ which fit the data on ρ, ω and ψ [8]. This fact is also the reason why other resonances higher than ψ''' are not considered here. Otherwise, $\hat{f}_V(\hat{m}_V^2)$ can be obtained from the data on leptonic width [11], that is

$$\hat{f}_V^2(\hat{m}_V^2) = \frac{27 \hat{m}_V^3}{16 \pi \alpha^2} \hat{\Gamma}(V \rightarrow \ell^+ \ell^-), \quad (16)$$

then $\hat{f}_V(0)$ would follow respectively as written in Tab. 1.

From Eqs. (7) and (8), it is obvious that $V_{uq}^* V_{ub}/V_{tq}^* V_{tb}$ would induce CP violation in the channel. For convenience, these terms can be collected as $(V_{uq}^* V_{ub}/V_{tq}^* V_{tb}) C_9^{\text{CP}}(\hat{s})$,

Parameter	Value
m_W	80.26 ± 0.16 (GeV)
m_Z	91.19 ± 0.002 (GeV)
m_u	0.005 (GeV)
m_d	0.139 (GeV)
m_c	1.4 (GeV)
m_b	4.8 (GeV)
m_t	175 ± 9 (GeV)
m_e	0.511 (MeV)
m_μ	105.66 (MeV)
m_τ	$1777^{+0.30}_{-0.27}$ (MeV)
μ	$5^{+5.0}_{-2.5}$ (GeV)
$\Lambda_{QCD}^{(5)}$	$0.214^{+0.066}_{-0.054}$ (GeV)
α_{QED}^{-1}	129
$\alpha_s(m_Z)$	0.117 ± 0.005
$\sin^2 \theta_w$	0.2325
m_{B^0}	5279.2 ± 1.8 (MeV)
τ_{B^0}	1.28 ± 0.06 (ps)
η_{QCD}	0.55
$\sqrt{f_{B_d}^2 B_{B_d}}$	173 ± 40 (MeV)
$\mathcal{B}(B \rightarrow X_c \ell \bar{\nu})$	$(10.4 \pm 0.4)\%$
x_d	0.73 ± 0.05

Table 2: The values of parameters used throughout the paper.

with

$$\begin{aligned}
C_9^{\text{CP}}(\hat{s}) &= (3C_1 + C_2 + 3C_3 + C_4 + 3C_5 + C_6) \\
&\times \left[g(\hat{m}_c, \hat{s}) - g(\hat{m}_u, \hat{s}) - \frac{16\pi^2}{9} \left(\sum_{V=\psi, \dots} F_V(\hat{s}) - \sum_{V=\rho, \omega} F_V(\hat{s}) \right) \right] \quad (17)
\end{aligned}$$

Now let me derive some relations in the CKM unitarity triangle and give numerical calculation for the auxiliary functions defined above. Especially it is worthwhile to see how large the contribution of C_9^{CP} . Using Wolfenstein parametrization [6], one can rewrite the CKM factor as

$$\frac{V_{uq}^* V_{ub}}{V_{tq}^* V_{tb}} \sim \begin{cases} \frac{r(e^{-i\gamma} - r)}{1 + r^2 - 2r \cos \gamma} & , \quad q = d \\ \lambda^2 r e^{-i\gamma} & , \quad q = s \end{cases} \quad (18)$$

As mentioned before, from Eqs. (4) and (18) it is obvious that in the $b \rightarrow s \ell^+ \ell^-$ decay, $u\bar{u}$ loop and then C_9^{CP} is less important and negligible. In general one

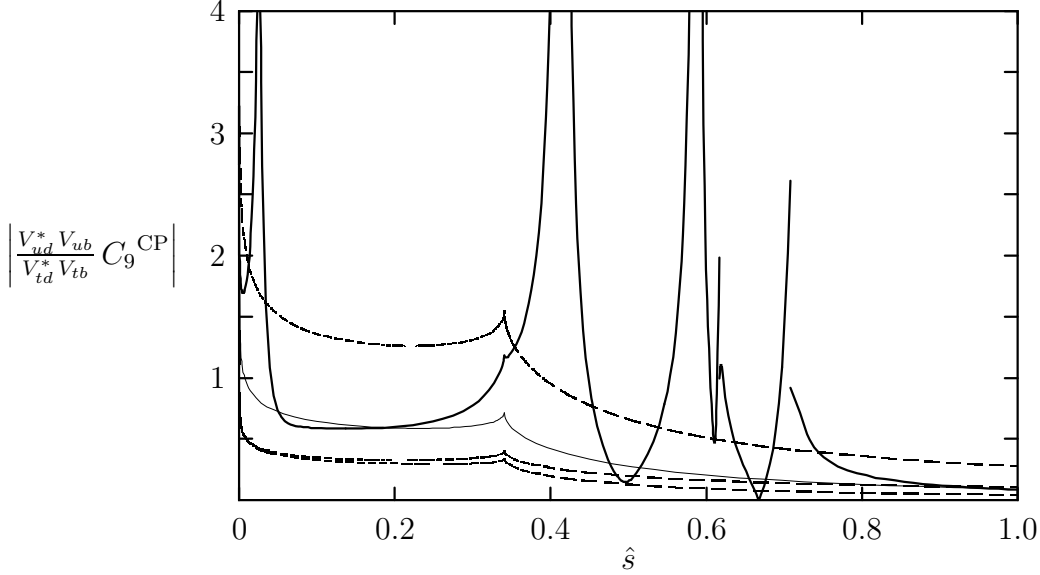


Figure 2: The magnitude of C_9^{CP} with (solid thick curve) and without (solid thin curve) resonances for $(\gamma, x) = (48.6^\circ, 0.778)$. The upper, middle and lower dashed curves show the magnitude without resonances for same x and $\gamma = 0^\circ, -90^\circ, 90^\circ$.

must treat r and γ as free parameters, while x must be determined by the data of $B_d^0 - \bar{B}_d^0$ mixing. However, in the SM the unitarity triangle is satisfied in a good approximation, so one can relate r and x each other as below

$$r = \sqrt{|x^2 - \sin^2 \gamma|} + \cos \gamma. \quad (19)$$

Here x is determined by the experimental value of x_d in the $B_d^0 - \bar{B}_d^0$ mixing, that is

$$x = \left[\frac{x_d}{G_F^2 / (6 \pi^2) m_{B_d} M_W^2 \tau_{B_d} \eta_{\text{QCD}} f_{B_d}^2 B_{B_d} |F_{\Delta B=2}|^2} \right]^{1/2}, \quad (20)$$

with [12]

$$F_{\Delta B=2} = \frac{4 - 15 x_t + 12 x_t^2 - x_t^3 - 6 x_t^2 \ln x_t}{4 (1 - x_t)^3}, \quad (21)$$

and $x_t = (m_t/m_W)^2$. For m_{B_d} and τ_{B_d} , I use m_{B^0} and τ_{B^0} .

The magnitude of $(V_{ud}^* V_{ub}/V_{td}^* V_{tb}) C_9^{\text{CP}}$ as a function of \hat{s} is depicted in Fig. 2. Here I use the following values for the Wilson coefficients

$$C_1 = -0.2404, C_2 = 1.1032, C_3 = 0.0107, C_4 = -0.0249, C_5 = 0.0072,$$

$$C_6 = -0.03024, C_7^{\text{eff}} = -0.3109, C_8 = -0.1478, C_9^{\text{NLO}} = 4.1990, C_{10} = -4.5399,$$

that are obtained by using the central values in Tab. (2), The solid curves show the magnitude for $(\gamma, x) = (48.6^\circ, 0.778)$ that is the best fit in the SM up to now and equivalent to $(\rho, \eta) = (0.3, 0.34)$. The upper, middle and lower dashed curves show the magnitude without LD effects with $\gamma = 0^\circ, -90^\circ, 90^\circ$. It is obvious that the contribution is significant, about $\sim 20\%$ of C_9^{NLO} at low \hat{s} region ($\hat{s} < 0.4$).

Now, I am ready to analyse the decay rate and asymmetries in the channel.

3 Decay rate and asymmetries

The double differential decay rate for semi-leptonic $B \rightarrow X_q \ell^+ \ell^-$ decay, involving the lepton and light quark masses, is expressed as

$$\begin{aligned} \frac{d^2 \mathcal{B}(\hat{s}, z)}{d\hat{s} dz} &= \mathcal{B}_o \sqrt{1 - \frac{4\hat{m}_\ell^2}{\hat{s}}} \hat{u}(\hat{s}) \left\{ 4 \left[|C_9^{\text{eff}}|^2 - |C_{10}|^2 \right] \hat{m}_\ell^2 \left[1 - \hat{s} + \hat{m}_q^2 \right] \right. \\ &\quad + \left[|C_9^{\text{eff}}|^2 + |C_{10}|^2 \right] \left[(1 - \hat{m}_q^2)^2 - \hat{s}^2 - \hat{u}(\hat{s})^2 \left(1 - \frac{6\hat{m}_\ell^2}{\hat{s}} \right) z^2 \right] \\ &\quad + 4 |C_7^{\text{eff}}|^2 \frac{1 + 2\hat{m}_\ell^2/\hat{s}}{\hat{s}} \\ &\quad \times \left[1 - \hat{m}_q^2 - \hat{m}_q^4 + \hat{m}_q^6 - \hat{s} (8\hat{m}_q^2 + \hat{s} + \hat{m}_q^2 \hat{s}) + \hat{u}(\hat{s})^2 (1 + \hat{m}_q^2) z^2 \right] \\ &\quad - 8 \text{Re} \left(C_9^{\text{eff}} \right)^* C_7^{\text{eff}} \left[1 + \frac{2\hat{m}_\ell^2}{\hat{s}} \right] \left[\hat{s} (1 + \hat{m}_q^2) - (1 - \hat{m}_q^2)^2 \right] \\ &\quad \left. + 4 C_{10} \left[\text{Re} \left(C_9^{\text{eff}} \right)^* \hat{s} + 2 C_7^{\text{eff}} (1 + \hat{m}_q^2) \right] \hat{u}(\hat{s}) z \right\}, \end{aligned} \quad (22)$$

where $\hat{u}(\hat{s}) = \sqrt{[\hat{s} - (1 + \hat{m}_q^2)^2][\hat{s} - (1 - \hat{m}_q^2)^2]}$, $z = \cos \theta$ is the angle of ℓ^+ measured with respect to the b -quark direction in the dilepton CM system and the normalization factor,

$$\mathcal{B}_o = \mathcal{B}(B \rightarrow X_c \ell \bar{\nu}) \frac{3 \alpha^2}{16 \pi^2} \frac{|V_{tq}^* V_{tb}|^2}{|V_{cb}|^2} \frac{1}{f(\hat{m}_c) \kappa(\hat{m}_c)}, \quad (23)$$

is to reduce the uncertainty due to b -quark mass. In the preceding notation, the CKM factor would read $|V_{td}^* V_{tb}|^2 / |V_{cb}|^2 \sim \lambda^2 x^2$. $f(\hat{m}_c)$ is the phase space function for $\Gamma(B \rightarrow X_c \ell \nu)$ in parton model, while $\kappa(\hat{m}_c)$ accounts the $O(\alpha_s)$ QCD correction

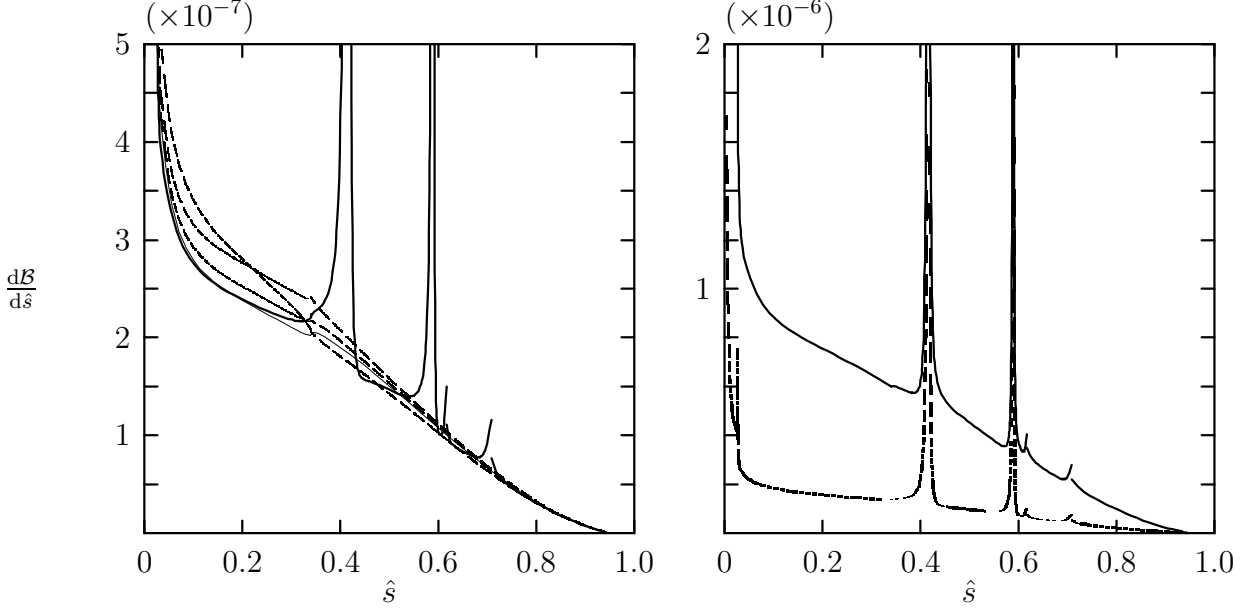


Figure 3: Left : differential BR for $e^+ e^-$ with (thick curve) and without (thin curve) resonances for $(\gamma, x) = (48.6^\circ, 0.778)$. The upper, middle and lower dashed curves show the SD contribution for same x and $\gamma = 0^\circ, 90^\circ, -90^\circ$. Right : same with the left for $\gamma = 48.6^\circ$ and $x = 1.368$ (solid curve) and 0.631 (dashed curve).

to the decay. Writing both functions explicitly,

$$f(\hat{m}_c) = 1 - 8\hat{m}_c^2 + 8\hat{m}_c^6 - \hat{m}_c^8 - 24\hat{m}_c^4 \ln \hat{m}_c, \quad (24)$$

$$\kappa(\hat{m}_c) = 1 - \frac{2\alpha_s(m_b)}{3\pi} \left[\frac{3}{2} + \left(\pi^2 - \frac{31}{4} \right) (1 - \hat{m}_c)^2 \right], \quad (25)$$

and using the values in Tab. 2, $f(\hat{m}_c) = 0.542$ and $\kappa(\hat{m}_c) = 0.885$.

3.1 Decay rate

Now, let me consider the dilepton invariant mass distribution of the differential branching-ratio (BR). It can be obtained by integrating Eq. (22) over the whole region of variable z ,

$$\frac{d\mathcal{B}(\hat{s})}{d\hat{s}} = \int_{-1}^1 dz \frac{d^2\mathcal{B}(\hat{s}, z)}{d\hat{s}dz}. \quad (26)$$

This gives

$$\begin{aligned} \frac{d\mathcal{B}(\hat{s})}{d\hat{s}} &= \frac{4}{3} \mathcal{B}_o \sqrt{1 - \frac{4\hat{m}_\ell^2}{\hat{s}}} \hat{u}(\hat{s}) \left\{ 6 \left[|C_9^{\text{eff}}|^2 - |C_{10}|^2 \right] \hat{m}_\ell^2 \left[1 - \hat{s} + \hat{m}_q^2 \right] \right. \\ &\quad \left. + \left[|C_9^{\text{eff}}|^2 + |C_{10}|^2 \right] \left[(1 - \hat{m}_q^2)^2 + \hat{s} (1 + \hat{m}_q^2) - 2\hat{s}^2 + \hat{u}(\hat{s})^2 \frac{2\hat{m}_\ell^2}{\hat{s}} \right] \right\} \end{aligned}$$

$$\begin{aligned}
& +4 \left| C_7^{\text{eff}} \right|^2 \frac{1 + 2 \hat{m}_\ell^2 / \hat{s}}{\hat{s}} \\
& \quad \times \left[2 (1 + \hat{m}_q^2) (1 - \hat{m}_q^2)^2 - (1 + 14 \hat{m}_q^2 + \hat{m}_q^4) \hat{s} - (1 + \hat{m}_q^2) \hat{s}^2 \right] \\
& + 12 \text{Re} \left(C_9^{\text{eff}} \right)^* C_7^{\text{eff}} \left[1 + \frac{2 \hat{m}_\ell^2}{\hat{s}} \right] \left[(1 - \hat{m}_q^2)^2 - (1 + \hat{m}_q^2) \hat{s} \right] \Big\} . \quad (27)
\end{aligned}$$

The distribution of differential BR on dilepton invariant mass for $B \rightarrow X_d e^+ e^-$ is given in Fig. 3 for various values of γ and x . High sensitivity on x is mostly coming from the CKM factor in Eq. (23), while the sensitivity on γ seems significant only in the low \hat{s} region. Then, in the high \hat{s} region the differential BR may be a good test for x and makes good the loss of $B_d^0 - \bar{B}_d^0$ mixing due to the theoretical uncertainties in the treatment of hadron matrix element $\langle B | \mathcal{O}^\dagger \mathcal{O} | B \rangle$. Anyway, I have checked that the momentum dependence of resonances in the channel is not as large as the result in [8]. There is only $\sim 4\%$ reduction compared with using $\hat{f}_V(\hat{m}_V^2)$ for all region. This is because the $1/\hat{s}$ suppression in Eq. (12) [9].

Next, I am going on examining some measurements that are sensitive on γ and less sensitive on x . This may be achieved by considering the asymmetries and normalizing them with the differential BR to eliminate the CKM factor.

3.2 Forward-backward asymmetry

First, I provide the FB asymmetry. The normalized FB asymmetry is defined as follows [13]

$$\bar{\mathcal{A}}_{\text{FB}}(\hat{s}) = \frac{\int_0^1 dz \frac{d^2 \mathcal{B}(\hat{s}, z)}{d\hat{s} dz} - \int_{-1}^0 dz \frac{d^2 \mathcal{B}(\hat{s}, z)}{d\hat{s} dz}}{\int_0^1 dz \frac{d^2 \mathcal{B}(\hat{s}, z)}{d\hat{s} dz} + \int_{-1}^0 dz \frac{d^2 \mathcal{B}(\hat{s}, z)}{d\hat{s} dz}} = \frac{d\mathcal{A}_{\text{FB}}(\hat{s})/d\hat{s}}{d\mathcal{B}(\hat{s})/d\hat{s}} . \quad (28)$$

Then, after integrating Eq. (27) properly, the nominator reads

$$\frac{d\mathcal{A}_{\text{FB}}(\hat{s})}{d\hat{s}} = -4 \mathcal{B}_o \sqrt{1 - \frac{4 \hat{m}_\ell^2}{\hat{s}}} \hat{u}(\hat{s})^2 C_{10} \left[\text{Re} \left(C_9^{\text{eff}} \right)^* \hat{s} + 2 C_7^{\text{eff}} \left(1 + \hat{m}_q^2 \right) \right] . \quad (29)$$

In Fig. 4, I plot the FB asymmetry for $B \rightarrow X_d e^+ e^-$ with and without the resonances in the left figure, while in the right one with varying γ and keeping x to be constant.

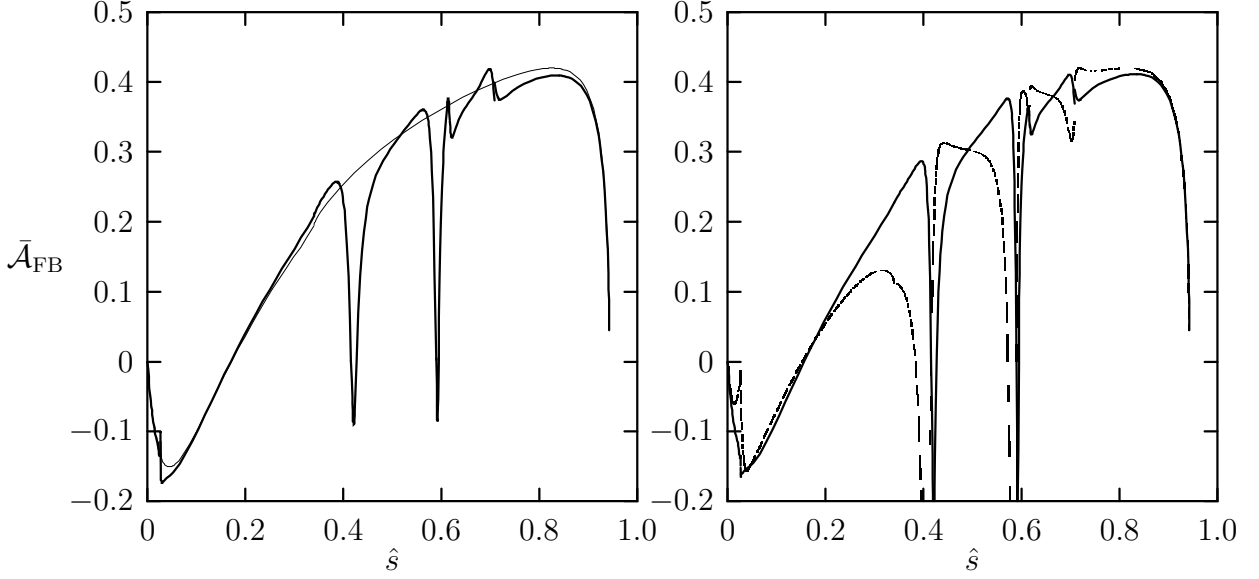


Figure 4: Left : FB asymmetry for $e^+ e^-$ with (thick curve) and without (thin curve) resonances for $(\gamma, x) = (48.6^\circ, 0.778)$. Right : same with the left for same x and $\gamma = 90^\circ$ (solid line) and 0° (dashed line).

3.3 CP asymmetry

Doing same treatment as [4] in the amplitude level, the normalized CP asymmetry can be written simply as

$$\bar{\mathcal{A}}_{\text{CP}}(\hat{s}) = \frac{d\mathcal{B}(\hat{s})/d\hat{s} - d\bar{\mathcal{B}}(\hat{s})/d\hat{s}}{d\mathcal{B}(\hat{s})/d\hat{s} + d\bar{\mathcal{B}}(\hat{s})/d\hat{s}} = \frac{-2 d\mathcal{A}_{\text{CP}}(\hat{s})/d\hat{s}}{d\mathcal{B}(\hat{s})/d\hat{s} + 2 d\mathcal{A}_{\text{CP}}(\hat{s})/d\hat{s}}, \quad (30)$$

where \mathcal{B} and $\bar{\mathcal{B}}$ denote the BR of $\bar{b} \rightarrow q \ell^+ \ell^-$ and its complex conjugate $b \rightarrow \bar{q} \ell^+ \ell^-$ respectively. For convenience, C_9^{eff} is divided to be two terms according to the factor

$V_{uq}^* V_{ub}/V_{tq}^* V_{tb}$ as below

$$C_9^{\text{eff}} = \bar{C}_9 + \frac{V_{uq}^* V_{ub}}{V_{tq}^* V_{tb}} C_9^{\text{CP}}. \quad (31)$$

Then, the result for the differential CP asymmetry is

$$\begin{aligned} \frac{d\mathcal{A}_{\text{CP}}(\hat{s})}{d\hat{s}} &= \frac{4}{3} \mathcal{B}_0 \sqrt{1 - \frac{4\hat{m}_\ell^2}{\hat{s}}} \hat{u}(\hat{s}) \text{Im} \left[\frac{V_{uq}^* V_{ub}}{V_{tq}^* V_{tb}} \right] \\ &\times \left\{ \text{Im} [\bar{C}_9^* C_9^{\text{CP}}] \left[(1 - \hat{m}_q^2)^2 + \hat{s} (1 + \hat{m}_q^2) - 2\hat{s}^2 + \hat{u}(\hat{s})^2 \frac{2\hat{m}_\ell^2}{\hat{s}} \right. \right. \\ &\quad \left. \left. + 6\hat{m}_\ell^2 (1 - \hat{s} + \hat{m}_q^2) \right] \right. \\ &\left. + 6 \text{Im} [C_7^{\text{eff}} C_9^{\text{CP}}] \left[1 + \frac{2\hat{m}_\ell^2}{\hat{s}} \right] \left[(1 - \hat{m}_q^2)^2 - (1 + \hat{m}_q^2) \hat{s} \right] \right\}. \quad (32) \end{aligned}$$

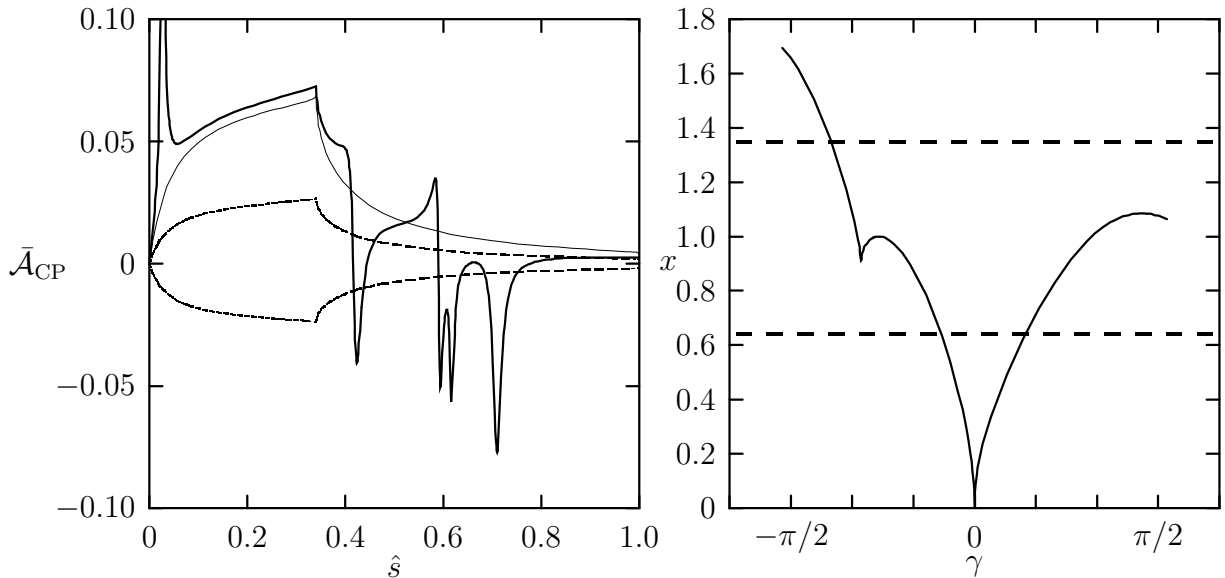


Figure 5: Left : CP asymmetry for $e^+ e^-$ with (solid thick curve) and without (solid thin curve) resonances for $(\gamma, x) = (48.6^\circ, 0.778)$. The upper and lower dashed curves show the SD contribution for same x and $\gamma = 90^\circ, -90^\circ$. Right : x as a function of γ where $\bar{\mathcal{A}}_{\text{CP}} = 0$. The dashed lines denote the upper and lower bounds of x in the SM.

In Fig. 5, I give the distribution of $\bar{\mathcal{A}}_{\text{CP}}$ (left figure) with (solid thick line) and without (solid thin line) resonances. It is easily understood that in the present case, the dependence on γ is large, because of the appearance of factor $r \sin \gamma$ from the CKM factor in Eq. (32). Moreover, it is clear that $\bar{\mathcal{A}}_{\text{CP}}$ will be non-zero if the imaginary part of Eq. (18) is non-zero. Anyway, a condition that $\bar{\mathcal{A}}_{\text{CP}} = 0$ for $q = d$ in the SM is satisfied by the following equation,

$$x^2 = \sin^2 \gamma \left[1 + \frac{1}{4} \left(1 - \sqrt{|3 + 4 \cot \gamma|} \right)^2 \right], \quad (33)$$

by using Eq. (19). The right figure in Fig. 5 is plotted based on this equation. As depicted in the figure, there are still allowed regions of γ where $\bar{\mathcal{A}}_{\text{CP}} = 0$. Notice again that from Eq. (18), $\bar{\mathcal{A}}_{\text{CP}}(B \rightarrow X_s \ell^+ \ell^-)$ would be $\sim 5\%$ of $\bar{\mathcal{A}}_{\text{CP}}(B \rightarrow X_d \ell^+ \ell^-)$ due to the suppression of λ^2 .

3.4 Lepton-polarization asymmetry

Until now, all of the measurements are less sensitive to the lepton mass. Next, I provide the LP asymmetry which must be considered for heavy dilepton final

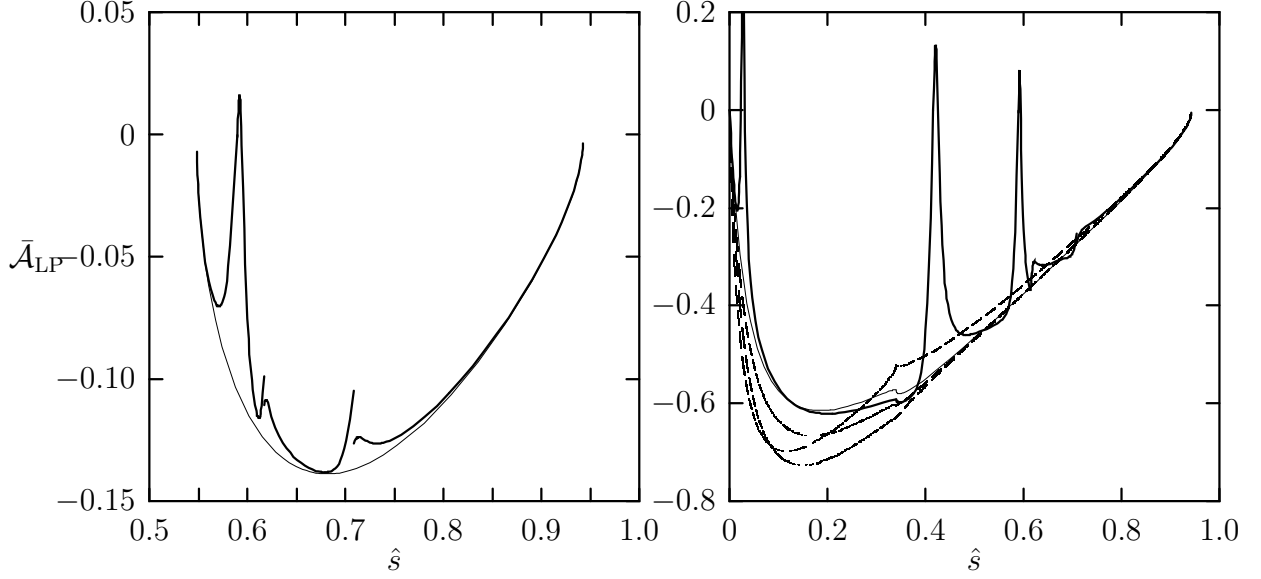


Figure 6: Left : LP asymmetry for $\tau^+ \tau^-$ with (solid thick curve) and without (solid thin curve) resonances for $(\gamma, x) = (48.6^\circ, 0.778)$. Right : same with the left but for $\mu^+ \mu^-$. The dashed curves show the SD contribution for same x and $\gamma = 0^\circ, 90^\circ, -90^\circ$.

state and is proposed first in [14] for $B \rightarrow X_s \tau^+ \tau^-$. Generally, the normalized LP asymmetry is given as

$$\bar{\mathcal{A}}_{\text{LP}}(\hat{s}) = \frac{d\mathcal{B}(\hat{s}, \mathbf{n})/d\hat{s} - d\mathcal{B}(\hat{s}, -\mathbf{n})/d\hat{s}}{d\mathcal{B}(\hat{s}, \mathbf{n})/d\hat{s} + d\mathcal{B}(\hat{s}, -\mathbf{n})/d\hat{s}} = \frac{d\mathcal{A}_{\text{LP}}(\hat{s})/d\hat{s}}{d\mathcal{B}(\hat{s})/d\hat{s}}, \quad (34)$$

with \mathbf{n} is a unit vector of any given spin direction of ℓ^- in its rest frame. Then, for the longitudinal polarization, that is \mathbf{n} has same direction with the momentum of ℓ^- (\mathbf{p}_{ℓ^-}),

$$\begin{aligned} \frac{d\mathcal{A}_{\text{LP}}(\hat{s})}{d\hat{s}} &= \frac{8}{3} \mathcal{B}_o \left(1 - \frac{4\hat{m}_\ell^2}{\hat{s}} \right) \hat{u}(\hat{s}) C_{10} \left\{ 6 C_7^{\text{eff}} \left[(1 - \hat{m}_q^2)^2 - \hat{s} (1 + \hat{m}_q^2) \right] \right. \\ &\quad \left. + \text{Re} \left(C_9^{\text{eff}} \right)^* \left[(1 - \hat{m}_q^2)^2 + \hat{s} (1 + m_q^2) - 2\hat{s}^2 \right] \right\}. \end{aligned} \quad (35)$$

The distribution is depicted in Fig. 6. As shown in the figure, for $\tau^+ \tau^-$ final state the sensitivity on γ is tiny. The reason is, for $\tau^+ \tau^-$ final state the distribution starts appearing in the region higher than $\hat{s} = (4\hat{m}_\tau^2)$, on the other hand, generally the high sensitivity on γ is expected in the low \hat{s} region. So it may be interesting to consider the transversal polarization that has different structure [14]. Unfortunately, I have checked that the transversal lepton polarization asymmetry is too small for

light dilepton like $\mu^+\mu^-$, then one must consider $\tau^+\tau^-$ again that the distribution is limited for higher \hat{s} region.

4 Summary

I have shown how to extract the angle γ of CKM unitarity triangle by the inclusive $B \rightarrow X_d \ell^+ \ell^-$ decay and the data of x_d in the SM. As the results, finally I can make some points as below.

1. For low \hat{s} region, i.e. $0.1 < \hat{s} < 0.3$, $5 \sim 10\%$ discrepancies in $\mathcal{B}(B \rightarrow X_d e^+ e^-)$ and $\bar{\mathcal{A}}_{\text{LP}}(B \rightarrow X_d \mu^+ \mu^-)$ may be good signals for the CP violation factor defined here.
2. According to the fact that the sensitivity on γ in the high \hat{s} region, i.e. $\hat{s} > 0.6$, is tiny, a measurement of x may be done by exploring one of the measurements discussed in the present paper in addition to the present data of x_d in $B_d^0 - \bar{B}_d^0$ mixing.
3. CP violation asymmetry in the channel should measure the dependence on γ . It will, at least, be a good probe to determine the sign of the angle γ .

To conclude, the measurements of the decay rate and asymmetries in $B \rightarrow X_d \ell^+ \ell^-$ decay will provide an independent information for γ . The information is a crucial test of CKM unitarity as well as leading to the discovery of unitarity violation.

Acknowledgements

I thank T. Muta for reading the manuscript, M. R. Ahmady and Y. Kiyo for useful discussion in q^- dependence in the long distance effects and D. X. Zhang for pointing out the $1/q^2$ dependence in the leptonic decay of vector mesons. I also would like to thank Particle Elementer Physics Group for the warm hospitality during my stay at ICTP Italy in the last part of the work and the Ministry of Education, Science and Culture (Monbusho-Japan) for the financial support.

References

- [1] A. Ali, talk given at 4th KEK Topical Conference on Flavor Physics in Tsukuba - Japan, and references therein.
- [2] B. Grinstein, M. J. Savage and M. B. Wise, *Nucl. Phys.* **B319** (1989) 271;
R. Grigjanis, P. J. O'Donnell, M. Sutherland and H. Navelet, *Phys. Lett.* **B223** (1989) 239.
- [3] A. V. Manohar and M. B. Wise, *Phys. Rev.* **D49** (1994) 1310;
A. Ali, G. Hiller, L. T. Handoko and T. Morozumi, *Phys. Rev.* **D55** (1997) 4105.
- [4] F. Krüger and L. M. Sehgal, *Phys. Rev.* **D55** (1997) 2799.
- [5] M. Jezabek and J. H. Kühn, *Nucl. Phys.* **B320** (1989) 20;
M. Misiak, *Nucl. Phys.* **B393** (1993) 23 [Err. **B439** (1995) 461];
A. J. Buras and M. Münz, *Phys. Rev.* **D52** (1995) 186.
- [6] L. Wolfenstein, *Phys. Rev. Lett.* **51** (1983) 1945.
- [7] C. S. Lim, T. Morozumi and A. I. Sanda, *Phys. Lett.* **B218** (1989) 343;
N. G. Deshpande, J. Trampetic and K. Panose, *Phys. Rev.* **D39** (1989) 1461;
P. J. O'Donnell and H. K. K. Tung, *Phys. Rev.* **D43** (1991) R2067;
P. J. O'Donnell, M. Sutherland and K. K. Tung, *Phys. Rev.* **D46** (1992) 4091.
- [8] K. Terasaki, *Nuo. Cim.* **66A** (1981) 475;
N. G. Deshpande, X. G. He and J. Trampetic, *Phys. Lett.* **B367** (1996) 362;
M. R. Ahmady, *Phys. Rev.* **D53** (1996) 2843.
- [9] C. D. Lü and D. X. Zhang, *Phys. Lett.* **B397** (1997) 279.
- [10] T. Inami and C. S. Lim, *Prog. Theor. Phys.* 65 (1981) 297.
- [11] Particle Data Group, *Phys. Rev.* **D54** (1996) 1.

- [12] B. A. Campbell and P. J. O'Donnell, *Phys. Rev.* **D25** (1989) 1982;
A. J. Buras and M. K. Harlander, in *Heavy Flavours* (World Scientific, 1992) p.
58, edited by A. J. Buras and M. Lindner.
- [13] A. Ali, T. Mannel and T. Morozumi, *Phys. Lett.* **B373** (1991) 505.
- [14] J. L. Hewett, *Phys. Rev.* **D53** (1996) 4964;
F. Krüger and L. M. Sehgal, *Phys. Lett.* **B380** (1996) 199.